Patterns of sulfur isotope fractionation during microbial sulfate reduction

PATTERNS OF SULFUR ISOTOPE FRACTIONATION BY SULFATE REDUCING BACTERIA

Alexander S. Bradley[1,*,†], William D. Leavitt[1,2,†], Marian Schmidt[2,3], Andrew H. Knoll[2,4], Peter R. Girguis[4], and David T. Johnston[2]

[1]*Department of Earth and Planetary Sciences, Washington University in St. Louis, 1 Brookings Drive, St. Louis MO, 63130*

[2]*Department of Earth and Planetary Sciences, Harvard University, 20 Oxford Street, Cambridge MA 02138*

[3]*Department of Ecology & Evolutionary Biology, University of Michigan, 830 North University, Ann Arbor, MI 48109*

[4]*Department of Organismic and Evolutionary Biology, Harvard University, 26 Oxford Street, Cambridge MA 02138*

*Correspondence to: *abradley at eps.wustl.edu*

†Authors contributed equally

Running title: Ecophysiology of SRB S-isotope fractionation

ABSTRACT

Studies of microbial sulfate reduction have suggested that the magnitude of sulfur isotope fractionation varies with sulfate concentration. Small apparent sulfur isotope fractionations preserved in Archean rocks have been interpreted as suggesting Archaean sulfate concentrations of less than 200 μM, while later larger fractionations have been interpreted to require higher sulfate concentrations. In this work, we demonstrate that isotope fractionation can sometimes vary with sulfate concentrations over a large range of concentrations, but that this relationship depends on the organism being studied. Two sulfate reducing bacteria grown in continuous culture between 0.1 and 6 mM sulfate showed markedly different relationships between sulfate concentration and isotope fractionation. *Desulfovibrio vulgaris* str. Hildenborough cultures showed a large and relatively constant isotope fractionation ($^{34}\varepsilon_{SO4\text{-}H2S} \cong 25‰$) over the experimental range of sulfate concentrations. Over the same concentration range, fractionation by *Desulfovibrio alaskensis* strain G20 strongly correlated with sulfate. Both data sets can be modeled as Michaelis-Menten (MM) type relationships but with very different MM constants, suggesting that the fractionations imposed by these organisms respond in dramatically different ways to sulfate concentrations.

These data reveal complexity in the sulfate concentration-fractionation relationship. Sulfur isotope fractionation during sulfate reduction relates to environmental sulfate concentrations but also to strain-specific physiological parameters such as the affinity of sulfate-reducing microorganisms for sulfate and electron donors. Previous studies have suggested that the relationship between sulfate concentration and isotope fractionation is best fit with a MM fit. suggested We present a simple model, grounded in the physiology of sulfate reduction, in which the ratio of MM relationships for sulfate and electron donor uptake produces the relationships seen in experimental studies: a MM relationship with sulfate concentration, and a hyperbolic relationship with growth rate.

Since both environmental and biological factors influence the fractionation recorded in geological samples, understanding their relationship is critical to interpreting the sulfur isotope record. As the acquisition machinery for sulfate and electron acquisition has been subject to selective pressure over Earth history, its evolution may complicate efforts to uniquely reconstruct ambient sulfate concentrations from a single sulfur isotopic composition.

Keywords: *co-limitation and threshold effects; Michaelis-Menten; marine sulfate concentration; Archean seawater*

INTRODUCTION

Evolution of the marine sulfate reservoir is a key parameter in modeling Earth's surface oxidation state through time (Berner and Canfield, 1989; Canfield, 2004). Today, seawater sulfate represents an oxidant reservoir ten times the size of atmospheric O_2 (Hayes and Waldbauer, 2006). One of the most powerful tools for understanding the evolution of the sulfate reservoir, and by proxy the surface sulfur cycle, is the ratio of stable sulfur isotopes in sulfur-bearing minerals found in marine sedimentary rocks. Marine sulfate concentrations are linked to geological isotope records largely via microbial metabolism, most notably by microbial sulfate reduction (MSR), a metabolic process that couples organic carbon or hydrogen oxidation to sulfate reduction. Details of isotopic records permit the quantification of seawater sulfate through Earth history, but such inferences are predicated on a fundamental understanding of the broad suite of factors that influence the fractionation of sulfur isotopes during MSR.

MSR can yield a large mass-dependent fractionation between sulfate and sulfide (Chambers et al., 1975; Harrison and Thode, 1958; Leavitt et al., 2013; Sim et al., 2011c); the product sulfide is depleted in heavy isotopes, leaving the residual sulfate enriched. Both environmental and physiological factors contribute to the expressed fractionation. For example, Habicht et al. (2002) presented data suggesting that $^{34}S/^{32}S$ fractionations greater than 5‰ are expressed only when ambient sulfate concentration exceeds 200 μM – approximately one percent of the modern seawater sulfate concentration. This concentration threshold is similar in magnitude to the sulfate half-saturation concentrations (K_s) associated with growth kinetics of some MSR strains (Pallud and Van Cappellen, 2006; Tarpgaard et al., 2011). When paired with Precambrian sedimentary sulfur isotope record, this fractionation threshold value was taken to imply an increase in seawater sulfate concentrations near the Archean – Proterozoic boundary, where a dramatic expansion of S-isotope fractionation is preserved (Habicht et al., 2002). This, in turn, suggests a strong physiological control on the geological isotope record (Habicht et al., 2002; Habicht et al., 2005; Szabo et al., 1950) and implies that as microbial physiologies are better understood, more refined geological storylines are possible.

Microbial physiology provides the context for mechanistically evaluating how low sulfate concentrations limit sulfur isotope fractionation. Extensive work on the sulfate uptake half-saturation constant (K_s) demonstrates a range of uptake capacities in natural communities and pure cultures alike (see compilations in (Pallud and Van Cappellen, 2006; Tarpgaard et al., 2011). For instance, it was originally intuited that microbes that evolved in and adapted to lacustrine environments with low ambient sulfate concentrations will have low K_s values, with the opposite posited for marine strains (Bak and Pfennig, 1991; Holmer and Storkholm, 2001). However, in natural samples, measured K_s values show no clear relationship with salinity; freshwater and marine sediments have apparently similar ranges of K_s (see review in Tarpgaard et al. (2011)). That said, low K_s values have been observed more frequently in freshwater cultures than in marine cultures (Tarpgaard et al., 2011). Further, Tarpgaard et al. (2011) demonstrate that individual microbial strains within a community can have different apparent K_s, values for sulfate, lessening the validity of using the realized K_s as a proxy for the all members of a given environment. This is also consistent with genomic analyses (Hauser et al., 2011; Heidelberg et al., 2004), which suggest that individual microbial strains may carry multiple sulfate transporters, possibly of varying sulfate K_s and V_{max} (maximal transport rate). Such complexity suggests that a single measure of cellular K_s is an imperfect guide to the concentration-dependence of fractionation. As such, the relationship between sulfate concentration/activity, transport, and isotope fractionation is likely more complex than a simple and universal sulfate concentration threshold value and related step-function change in sulfur isotope fractionation.

It should also be noted that sulfate transporters enable sulfate-reducing microorganisms to compete for sulfate as a function of both the cellular half-saturation constant, K_s, and of the maximum rate of cellular sulfate uptake, $V_{max.}$ It is important to appreciate that V_{max} itself is also a function of the number and characteristics of sulfate ion transporters in the cell membrane (Aksnes and Egge, 1991). Much work suggests that the appropriate parameter to describe the cellular uptake efficiency for any ion – including sulfate – is the affinity parameter A_s, which is V_{max} /K_s (Aksnes and Egge, 1991; Button, 1985; Healey, 1980; Smith et al., 2009). This term captures the influence of both the maximal rate of transport and the half-saturation constant. As strains with a higher A_s are able to import sulfate more efficiently into the cell, the opportunity for isotope fractionation should increase; at low transport velocities (i.e. sulfate import rates),

transported sulfate is likely to be quantitatively reduced to sulfide, which due to mass balance would minimize isotopic fractionation.

In this study we report results from two sets of continuous-culture experiments, each employing an axenic strain of sulfate-reducing bacteria. We examine pure strains rather than enrichment cultures or diverse sedimentary communities in order to avoid complexities introduced by multiple competing strains, each with potentially different sulfate affinities and transport kinetics. In each set of experiments, the bacterial population was cultivated at steady state under a range of different sulfate concentrations (0.1 to 6 mM) in order to assay the relationship between sulfate concentration and isotope fractionation. The freshwater (*Desulfovibrio vulgaris* str. Hildenborough) and marine (*Desulfovibrio alaskensis* str. G20) strains selected are among the most well studied sulfate reducers (Hansen, 1994; Pereira et al., 2011; Wall et al., 1993). Each strain has a fully sequenced genome (Hauser et al., 2011; Heidelberg et al., 2004), is genetically tractable, and is biochemically well-characterized (Grein et al., 2013; Venceslau et al., 2014), providing a wide range of tools for follow-up investigations.

To date, previous physiological work has reported one sulfate K_s for *D. vulgaris* at 0.032 mM (Ingvorsen and Jørgensen, 1984). The genome of *D. vulgaris* (http://www.ncbi.nlm.nih.gov) further contains three annotated sulfate transport proteins. In contrast, *D. alaskensis* has no reported K_s; however, closely related strains have values ranging from 0.005 mM to greater than 0.250 mM (Dalsgaard and Bak, 1994; Fukui and Takii, 1994; Okabe et al., 1992). The *D. alaskensis* genome contains at least 10 sulfate transporters; unknown transport proteins are also present and may increase this estimate. Such redundancy is consistent with the notion that a range of sulfate affinities can be exhibited in a single strain or environment (Tarpgaard et al., 2011). Here we present the experimental design and results, consider potential physiological and environmental factors that can explain the observed differences, and discuss the ramifications of these data on interpretations of the geological sulfur isotope record.

MATERIALS AND METHODS SUMMARY

Each strain (*D. alaskensis* and *D. vulgaris*) was grown in stirred continuous culture vessels held at room temperature (25 °C) for roughly 40 days. We employed a continuous flow bioreactor to avoid the complexities of closed-system Rayleigh distillation effects incurred during growth in batch culture (Leavitt et al., 2013). In continuous culture at steady state, concentration of the limiting substrate (in this case, lactate) remains invariant and is a function of dilution rate; the growth rate (μ, day^{-1}) is also constant and equal to the dilution rate (D, day^{-1}). This design allowed us to match *D. vulgaris* and *D. alaskensis* growth rates at 0.037 ± 0.003 and 0.034 ± 0.001 (days^{-1}), respectively. Growth rate and biomass yield were modulated with lactate as the limiting substrate. Any variability recorded in these experiments should, thus, primarily reflect the isotopic response to changing sulfate concentrations. Our approach allows us to measure the fractionation behavior of MSR at constant growth rates over a range of sulfate concentrations (0.1 to 6.1 mM).

Sulfate and lactate were supplied to the bioreactors at rates necessary to achieve media concentrations from 0.5 to 10 mM. As the limiting nutrient, standing lactate concentrations in the chemostats were a function of dilution rate. The reactor vessel was continuously purged with a pre-conditioned (O_2-free and hydrated) anaerobic gas mixture (N_2:CO_2, 90:10), which also served to carry gas phase sulfide out of the reactor to a series of zinc acetate traps. Reactor pH was maintained at 7.0±0.02 via a pH-probe activated titration pump, which dosed either 1M HCl or 1M NaOH as appropriate (N_2-degassed and autoclave-sterilized). From the effluent, concentrations of lactate/acetate and sulfate/sulfide were measured daily along with optical density and all (gas and liquid) flow rates. Our reported concentrations are those measured from the chemostat effluent, and represent the effective concentration of sulfate in the reactor. Steady-state sulfate concentrations were measured directly from the bioreactor effluent, and represent the concentration available to the population (lower than the concentration of the inlet media). The fractionations of interest ($^{34}\varepsilon$ and $^{33}\lambda$) are thus between reactant sulfate and product sulfide, both collected from the effluent. For isotopic analysis, all samples were measured for $\delta^{34}S$ via SO_2 and select samples were fluorinated to SF_6 and measured for high precision $\delta^{33}S$ analysis (Johnston et al., 2005). Carbon and sulfur mass balances were always satisfied to within 2%. Growth rate was determined given growth data (cells/mL *or* A600/mL) with respect to the dilution rate (D, day^{-1}), and only samples satisfying a steady-state flow regime (*see*

Supplemental Information) were included in the final analysis. All chemical, biological, and isotopic methods are described in the supplemental materials.

RESULTS AND DISCUSSION

CHEMOSTAT EXPERIMENTS

The isotopic fractionation between sulfate and sulfide is plotted in Figure 1 as a function of the standing sulfate concentration in the chemostat for both *D. vulgaris* and *D. alaskensis*. Experiments with *D. vulgaris* yielded a range of $^{34}\varepsilon_{D.vulgaris}$ from 18.0 to 32.7‰ over the targeted sulfate concentrations. Specifically, $^{34}\varepsilon_{D.vulgaris}$ shows no significant covariance between sulfate concentration and fractionation (p = 0.19), meaning that there is no first-order dependence of fractionation on sulfate concentration between 0.1 and 5 mM. Furthermore, *D. vulgaris* demonstrates the capacity for significant isotope fractionation ($^{34}\varepsilon_{D.vulgaris}$ greater than 25‰, although with significant scatter) at sulfate concentrations as low as 0.1 mM. These data are consistent with a Michaelis-Menten type relationship between substrate concentration and fractionation (Habicht et al., 2005), with a $K_{m\text{-}frac}$ = 0.0027 mM (95% CI is 0 to 0.036 mM) and $^{34}\varepsilon_{max}$ = 25.8‰ (95% CI is 23.4 to 28.3‰). $K_{m\text{-}frac}$ is defined as the sulfate concentration at which expressed fractionation is one-half of the maximum fractionation under constant conditions excepting variable sulfate concentrations (Habicht et al., 2005).

In contrast, experiments with strain *D. alaskensis* produce a $^{34}\varepsilon_{D.alaskensis}$ that varies systematically from near 0 to 13‰ as steady-state sulfate concentrations are increased. These data show strong co-variance, via the linear regression model: $^{34}\varepsilon = (2.2 \pm 0.1)*[SO_4^{2-}] + (1.2 \pm 0.3)$, with a p-value less than 0.001. This result is consistent with a first-order dependence of $^{34}\varepsilon_{D.alaskensis}$ on sulfate concentration over the range tested (0.1 to 6.1 mM). The data could also be fit with a Michaelis-Menten type relationship, with a half-saturation constant of $K_{m\text{-}frac}$ = 8.9 mM (95% CI is 2.2 to 15.7 mM) and $^{34}\varepsilon_{max}$ of 34.5‰, 95% CI is 16.8 to 52.3 ‰). Although comparison of the two models using a corrected Akaike's (AIC_c) information criterion favors the linear model (62% likelihood), mechanistic considerations (*see* 'Evaluation of cellular K_s') suggest that the Michaelis-Menten formulation is preferable. Taking the *D. vulgaris* and *D. alaskensis* experiments together, the strains exhibits strikingly different patterns in both the

magnitude of $^{34}\varepsilon$ and its dependence on ambient sulfate concentration (i.e. the Michaelis-Menten fitting parameters).

The relationship between sulfate concentration and isotopic fractionation ($^{34}\varepsilon$) described above and elsewhere (Habicht et al., 2002; Habicht et al., 2005) can be extended to include ^{33}S. These data are presented in Figure 2 using two complementary minor isotope notations[§]: $^{33}\lambda$ and $\Delta^{33}S$. The $\Delta^{33}S$ notation is common in geological applications and is the deviation (in ‰ units) from a theoretical reference frame defined using the calculated low temperature thermodynamic equilibrium relationship between ^{32}S, ^{33}S, and ^{34}S where $^{33}\lambda = 0.515$. However, since $^{33}\lambda$ is not constant across various processes a calculation of its value provides another measure of minor isotope variance – it can be envisioned as approximately the slope of the curve on a plot of $\delta^{33}S$ vs. $\delta^{34}S$. Non-equilibrium processes can have slopes different than 0.515, most commonly less than 0.515 (Farquhar et al., 2003; Johnston et al., 2007). As both terms are widely used, we plot both $\Delta^{33}S$ and $^{33}\lambda$ versus $^{34}\varepsilon$ (Fig. 2).

Previous studies targeting $^{33}\lambda$ in open-system MSR experiments suggest that $^{33}\lambda$ varies linearly with $\delta^{34}S$ as a function of metabolic rate (Sim et al. 2011; Leavitt et al. 2013(Wu and Farquhar, 2011)). As these slopes carry a metabolism-specific component (Johnston et al 2005), the inclusion of ^{33}S extends the biogeochemical utility of S isotopes. Including ^{33}S allows the effects of sulfate reduction to be discerned from those of sulfide oxidation or sulfur disproportionation. For example, the $^{34}\varepsilon_{D.alaskensis}$ values (0-13‰) expressed in our experiments by strain *D. alaskensis* are not unique to MSR, as sulfide oxidation reactions often produce $^{34}\varepsilon$ less than 10‰. However, the inclusion of ^{33}S provides an additional isotopic constraint that can be used to trace the origin of sulfate and sulfide (Johnston et al., 2005). In our experiments, $\Delta^{33}S$ and $^{33}\lambda$ both show a strong relationship with $^{34}\varepsilon$ (Fig. 2), and for $\Delta^{33}S$: $\Delta^{33}S = (0.0031 \pm 0.0003)*(^{34}\varepsilon) + (0.20 \pm 0.01)$, *p*-value less than 0.0001. In this case AIC_c favors a Michaelis-Menten type fit (89% likelihood) with a $K_{m\text{-}frac} = 20.1$‰ [7.6 to 32.6 ‰] and $\Delta^{33}S_{max} = 0.169$ ‰, (95% CI 0.110 to 0.228 ‰). The $^{33}\lambda$ – $^{34}\varepsilon$ results for *D. alaskensis* and *D. vulgaris* fit within the context of previous work in which $^{33}\lambda_{MSR}$ (dimensionless) spans a range from 0.508 to 0.514

[§] We use standard isotope notation, where $\delta^{3x}S$ is the ratio of ^{3x}S to ^{32}S in a sample relative to a standard. We use $^{34}\varepsilon$ to capture the isotopic difference between sulfate and sulfide (=[$^{34}\alpha$ -1] 1000). Minor isotope notation includes $\Delta^{33}S$ (=$\delta^{33}S + 1000[\delta^{34}S/1000 +1]^{0.515}$ -1), which relates a composition to a theoretical reference line, and $^{33}\lambda$ (=ln[$^{33}\alpha$]/ln[$^{34}\alpha$]), which is approximately the slope of the tangent to the curve of $\delta^{33}S$ vs. $\delta^{34}S$.

(Farquhar et al. 2003; Johnston et al. 2005; 2007; Sim et al. 2011; Leavitt et al. 2013). In contrast, sulfide oxidation and sulfur disproportionation reactions result in $^{33}\lambda$ greater than 0.5145 (Johnston et al., 2005; Zerkle et al., 2009). Therefore, these data support minor sulfur isotopes as a quantitative indicator of specific metabolism, despite control on fractionation of other experimental parameters like sulfate (e.g., temperature, MSR strain, etc.).

EVALUATION OF CELLULAR K_S AS A PREDICTOR OF FRACTIONATION

These experiments demonstrate that different strains of sulfate reducing bacteria can show distinct relationships between sulfate concentration and isotope fractionation. The observed differences prompt a reexamination of previous data and reinvigorate the search for similar patterns. Harrison and Thode (1958) demonstrated a correlation between sulfate concentration and sulfur isotope fractionation with *D. desulfuricans*. More recent work using modified flow-through reactors (Habicht et al., 2002) and a recirculating chemostat (Habicht et al., 2005) shows a relationship in which $^{34}\varepsilon$ increases with sulfate concentration, and can be interpreted as asymptotically approaching a maximum value. This later work targeted the MSR *Archaeoglobus fulgidus*, a hyperthermophilic Archaea. In those studies, growth and cell specific sulfate reduction rate (csSRR) were controlled through organic carbon limitation, and the threshold effect of sulfate concentrations (i.e., a step function) was observed. The authors modeled this asymptotic behavior with an equation identical in form to a Michaelis-Menten equation although a linear fit to these data cannot be excluded without a theoretical justification (see below). The half-saturation constant in this fractionation equation ($K_{\text{m-frac}}$) is then defined as the concentration of sulfate at which the modeled fractionation was one-half the maximum fractionation. The value of $K_{\text{m-frac}}$ for sulfate was similar in magnitude to the Michaelis-Menten half-saturation constant (K_s) for sulfate-limited growth. The similarity in these constants inspired the proposition that $K_{\text{m-frac}}$ and K_s are directly (linearly) related, implying that the half saturation constant carries an isotopic – and perhaps geologic – fingerprint (Habicht et al., 2002).

A Michaelis-Menten -like mathematical relationship correctly predicts the fractionation pattern displayed by *D. vulgaris*. Previous work indicates a K_s for sulfate in *D. vulgaris* near 0.03 mM (Ingvorsen and Jørgensen, 1984), well below the sulfate concentrations in our experiments. If $K_{\text{m-frac}}$ is of a similar magnitude, as predicted by our measurements at millimolar sulfate, then at our minimum sulfate concentration of 0.1 mM, we expect to observe more than

90% of the maximum fractionation under the specific experimental conditions (i.e. csSRR and chemostat dilution rate) employed (Fig. 1; *see* Materials and Methods). Only a modest increase in fractionation would accompany further increases in sulfate concentrations, consistent with our observations for *D. vulgaris*. Changes in csSRR would have more dramatic consequences.

In contrast, a Michaelis-Menten-like equation can only explain the experimental results for strain *D. alaskensis* if the $K_{\text{m-frac}}$ is quite large - greater than the experimental window investigated here ($K_{\text{m-frac}}$ = 8.9 mM, 95% CI is 2.2 to 15.7 mM). We are unaware of any published sulfate K_s values from strain *D. alaskensis* specifically, although K_s values from related strains (*D. desulfuricans*) are consistently less than 0.5 mM (Tarpgaard et al., 2011) – eighteen-fold lower than would be required if $K_{\text{m-frac}}$ and K_s are to be similar. Given that the *D. alaskensis* genome contains at least 10 putative sulfate transporters, the cellular K_s for sulfate is likely highly dependent on growth conditions. One plausible explanation for the observed result is that under these conditions *D. alaskensis* expresses only low affinity sulfate transporters, and that a functional relationship between K_s and $K_{\text{m-frac}}$ holds. Indeed, a sulfate K_s of this magnitude is within the upper limits of published K_s values for sulfate (Fukui and Takii, 1994; Ingvorsen et al., 1984; Pallud and Van Cappellen, 2006; Roychoudhury, 2004; Tarpgaard et al., 2011).

These new data highlight the fact that the relationship between cellular K_s for sulfate and isotope fractionation remains unclear, and affinity (A_s) may be a more appropriate term to use when examining MSR in the context of environmental conditions. While K_s values for sulfate are directly related to the kinetics of growth under sulfate-limited conditions, experiments on the fractionation of sulfur isotopes are generally executed under electron donor limitation or co-limitation of sulfate and electron donor (e.g., this study, Habicht et al. 2002, 2005). Growth and sulfate reduction rates are therefore directly related to the affinity (A_s) for the electron donor relative to that of sulfate, rather than simply sulfate concentrations. Sulfate K_s pertains only to the cellular half-saturation constant for sulfate and may affect fractionation, particularly when sulfate is *not* growth-limiting. In more detail, sulfate transport in sulfate-reducing microorganisms is strictly regulated, and is accomplished via numerous possible mechanisms. These include H^+ and Na^+ symporters, which rely on concentration gradients and do not require ATP (Cypionka, 1995), whereas there also exist ATP-dependent ABC-type active transporters that pump sulfate into the cell against a concentration gradient (Piłsyk and Paszewski, 2009) and

are homologous to enzymes for assimilatory sulfate transport in other (non-sulfate-reducing) microorganisms. Energetic considerations favor the symporters as the primary transport mechanism for dissimilatory metabolism (Cypionka, 1995). Regulation of various transporters with different affinities (Cypionka, 1995; Tarpgaard et al., 2011) probably allows the cells to adapt to various sulfate concentrations; with high-affinity transporters up-regulated at low sulfate concentrations and vice versa. Therefore, one plausible explanation for the apparently divergent patterns in Fig. 1 is that transport mechanisms differ between *D. vulgaris* and *D. alaskensis*. For example, if under similar conditions *D. vulgaris* expressed high affinity sulfate transporters, its intracellular concentration of sulfate could remain elevated and allow fractionation to be maximized. The pattern seen in *D. alaskensis* may reflect lower affinity transporters, or a variation in the affinity of expressed transporters as sulfate concentrations are changed. There may, of course, be other differences in each strain's ability to import sulfate and electron donors that are not represented herein, and future studies should be designed to interrogate the means by which these and other strains acquire sulfate over a range of environmentally relevant conditions.

Since it has been demonstrated that fractionation is a function both of sulfate concentration (Habicht et al., 2002) and specific sulfate reduction rate (Chambers and Trudinger, 1975; Harrison and Thode, 1958; Leavitt et al., 2013; Sim et al., 2011c), it would be useful to understand the interaction of these two variables. Both can be related to the cellular machinery for sulfate reduction by comparing the independent rates of sulfate and electron supply to the cell (Bradley et al., 2011). Sulfur isotope fractionation will be maximized when intracellular sulfate concentrations are unlimited and electron supplies are limited. This is the situation that occurs at very low growth rates: electron donor limits the growth rate, but if sulfate is not limiting then cellular transport of sulfate should not be limiting either. We can conceptualize this growth state as a high supply of sulfate relative to electrons.

Conversely, sulfur isotope fractionation will be minimized if sulfate supply is limiting. If cells are able to obtain sufficient electrons to quantitatively reduce sulfate to sulfide, then expressed fractionation will be zero. This situation occurs when cells import electrons (via electron donors) sufficiently quickly that all imported sulfate is reduced to sulfide. The relationship between sulfur delivery and electron delivery is mechistically expressed at key enzymes in the sulfate reduction pathway. For example, the enzyme dissimilatory sulfite

reductase requires three components to function (Figure 4): i) electrons, delivered via an intracellular electron carrier, ii) sulfite

Therefore, to a first order fractionation is proportional to the rate at which sulfate can be imported into the cell, and inversely proportional to the rate at which electrons are imported into the cell.

[1] $$^{34}\varepsilon \sim \frac{\nu_{sulfate}}{\nu_{electrons}}$$

where $^{34}\varepsilon$ is the expressed fractionation, $\nu_{sulfate}$ is the rate at which sulfate is supplied to the cell. This rate is dependent on the kinetics of sulfate transporters, and is classically approximated as an Michaelis-Menten relationship:

[2] $$\nu_{sulfate} = \frac{V_{max}^{sulfate}[SO_4^{2-}]}{K_s^{sulfate} + [SO_4^{2-}]}.$$

The rate of sulfate reduction is similarly controlled, in a cell with excess sulfate, by the rate of electron supply to the reduction machinery. The rate that electron donors are imported can similarly be modeled as a Michaelis-Menten relationship, with different kinetic parameters for different electron donors. However, for the purposes of understanding fractionation the important parameter is the rate that electrons are supplied for the reduction of sulfate. This rate is proportional to the cell-specific sulfate reduction rate:

[3] $$\nu_{electrons} \sim csSRR$$

Combining these two relationships, the observed fractionation is proportional to the MM relationship for sulfate import, times the inverse of the cell-specific sulfate reduction rate.

[4] $$^{34}\varepsilon \sim \frac{V_{max}^{sulfate}[SO_4^{2-}]}{K_s^{sulfate} + [SO_4^{2-}]} \frac{1}{csSRR}$$

This relationship has two consequences, both of which have been demonstrated empirically: first, at a given csSRR the relationship between sulfate concentration and sulfur isotope fractionation follows a curve that can be represented as a Michaelis-Menten curve (Habicht et al., 2005); second, at a given sulfate concentration the relationship between csSRR and fractionation is a nonlinear (hyperbolic) function of csSRR (Desmond-Le Quéméner and Bouchez, 2014; Leavitt et al., 2013; Sim et al., 2011c; Wing and Halevy, 2014). This equation can be related to that given by Habicht et al. (2005), where

[5] $$^{34}\varepsilon = \frac{\varepsilon_{max}[SO_4^{2-}]}{K_{m-frac} + [SO_4^{2-}]} = \frac{V_{max}^{sulfate}[SO_4^{2-}]}{K_s^{sulfate} + [SO_4^{2-}]} \frac{\gamma}{v_{SRR}}$$

and where γ represents a factor for the conversion from rate to fractionation; this may differ from one strain to another. In this formulation K_s and $K_{m\text{-}frac}$ are related, but distinct, values and the relationship between them depends on both the strains involved and the csSRR. In this formulation, ε_{max} (and therefore γ) is a function of csSRR, with a maximum value at low rates resulting in a fractionation equivalent to the thermodynamic equilibrium fractionation factor between sulfate and sulfide.

Given a single strain and concentration of electron donor, as is the case with our chemostat experiments, sulfate reduction rate is invariant, and the variation in fractionation would approximate a Michaelis-Menten curve on sulfate concentration, as shown by Habicht et al. (2005) (Figure 5A). Moreover, the apparent $K_{m\text{-}frac}$ need not be the same from strain to strain, and this is reflected in the data herein on *D. vulgaris* and *D. alaskensis* at the same SRR. The value primarily depends on both the strain-specific half-saturation constant for sulfate and the kinetic parameters related to transport of the electron donor. High sulfate concentrations and low growth rates (as limited by electron donor) both drive fractionations towards maximum (equilibrium-like) values. At constant sulfate concentrations, the relationship between fractionation and csSRR would have the hyperbolic relationship shown in Figure 5B and demonstrated in previous studies (Leavitt et al., 2013; Sim et al., 2011c). This hyperbolic relationship is conceptually similar to the relationship between carbon dioxide concentrations and $^{13}\varepsilon$ discrimination against carbon isotopes demonstrated during carbon assimilation (Laws et al., 1995; Popp et al., 1998). However, that is a linear relationship since CO_2 assimilation and growth rate are directly related.

FACTORS GOVERNING S ISOTOPE FRACTIONATION BY SRB

We propose that controls on S isotopic fractionation can generally be divided into four regimes, only a subset of which have been the foci of experimental research to date (Figure 6). Within each regime, transport and physiological factors will affect observed fractionation.

Sulfate limitation: in this regime, sulfate (terminal electron acceptor) availability limits the rate of sulfate reduction. Due to quantitative, or near-quantitative reduction of sulfate,

expressed fractionation is small or may even carry a small inverse isotope effect (Harrison and Thode, 1958).

Electron donor limitation: In this case, both sulfate concentration and csSRR are relevant to determining fractionation factors. At lower sulfate concentrations this parameter is still influential on fractionation so long as sulfate is not being quantitatively reduced (Regime I), while at higher sulfate concentrations (28mM, i.e. higher than two times the $K_{\text{m-frac}}$), rate is primarily determined by electron donor availability. This is the regime that is the focus of most studies on the magnitude of sulfur isotope fractionation (Chambers and Trudinger, 1975; Kaplan and Rittenberg, 1964; Leavitt et al., 2013; Sim et al., 2011a; Sim et al., 2011c).

Substrate co-limitation: Concentrations of both sulfate and electron donor are low relative to the cellular affinities. Growth rate in this case may be a second-order function that relates to the concentration and affinity of both substrates, or it may be the minimum growth rate predicted by either parameter (Liebig's law: (Saito et al., 2008)). Under these conditions, the expressed fractionation is likely to be a compound function of physiology and environment – making fractionation difficult to uniquely predict. Moreover, large fractionations are not excluded from this regime (Wing and Halevy, 2014), and significant fractionations have been observed at low sulfate concentrations (Canfield et al., 2010; Crowe et al., 2014; Gomes and Hurtgen, 2013; Nakagawa et al., 2012). If limitation of one constituent exerts ultimate control, then the system reverts to regime 1 or 2.

Nutrient or physical limitation(s): There can be other nutrients or factors – such as nitrogen, iron, or phosphorous limitation (Sim et al., 2012), a physical factor (e.g. temperature,(Canfield et al., 2006; Johnston et al., 2007)) or an intrinsic organismal factor that limits growth rate and fractionation. The rate—fractionation relationship has been demonstrated for electron donor/acceptor (Canfield, 2001; Chambers et al., 1975; Kaplan and Rittenberg, 1964; Leavitt et al., 2013; Sim et al., 2011a; Sim et al., 2011c) and for nutrients (Sim et al., 2012), and can plausibly extend to other parameters. Where growth rates are controlled by factors intrinsic to the cell (e.g. in most batch culture experiments, during early log-phase growth), expressed fractionations are likely to reflect rates of intracellular electron transport to electron-accepting sulfur intermediates, described above (Bradley et al., 2011). Under severely limited conditions it may be possible to approach equilibrium isotope fractionations (Wing and Halevy, 2014).

These regimes indicate that multiple interactions ultimately control the sulfur isotope fractionation expressed by any given organism in any particular environment. As mentioned above, one physiological component not yet explored is the potential for organisms to carry multiple sulfate uptake machineries of varying affinities. For example, as sulfate is consumed through a typical marine sedimentary early diagenetic profile (Jorgensen, 1979), the sulfate concentrations available for MSR vary from 28 to less than 1 mM. Possessing high affinity sulfate transporters may confer a selective advantage at low concentrations, whereas low affinity transporters may confer an advantage at high ambient sulfate. A recent study identified both high and low affinity uptake mechanisms through a sulfate-methane transition zone profile in marine sediments (Tarpgaard et al., 2011), showing that large differences in affinity are possible even within the microbial community from a specific environment. Optimization of cellular machinery for the acquisition of metabolites is observed in other metabolic processes. For example, carbon fixation by RuBisCO is optimized to intracellular CO_2/O_2 ratios (Tcherkez et al., 2006). The genome of *D. vulgaris* (Heidelberg et al., 2004) contains three annotated sulfate transport proteins, while the genome of *D. alaskensis* contains at least ten (Hauser et al., 2011). This redundancy is consistent with a potential range of affinities and could be further extended if unknown transport proteins are also present. In a microbial community with a mixture of organisms, each with a potential range of transporters, the overall observed fractionation will depend on how each member of the community processes sulfate and discriminate against its heavier isotopes.

An apparent range in affinities of enzymatic machinery for sulfate sets in place a prediction for an affinity continuum at the organismic level. The V_{max}/K_s expressed under any set of conditions is physiologically dependent and may incorporate feedbacks sensitive to sulfate concentration. The presence of both high and low affinity uptake mechanisms, at the cellular and community scales, is relevant to interpretation of the geochemical record. Continuing research will need to identify the full genetic and enzymatic controls on sulfate affinity in a variety of organisms, as well as the selective pressures to which these controls respond. In the future, more robust geochemical interpretations of sulfur isotopes may be achieved by furthering our understanding of how sulfate affinity has evolved in response to changing marine redox conditions and oxidant budgets (i.e. sulfate availability due to oxidative weathering), and how this evolution has influenced the sulfur isotope record. A high affinity for sulfate would have

been particularly advantageous early in Earth history, with the requirement becoming more relaxed as the Earth's surface became more oxidizing and sulfate more plentiful. That is, natural selection has likely altered dominant patterns of sulfur isotope fractionation over the course of Earth history. A genomic memory of ancient high affinity machinery may still be present in modern lacustrine environments, or other factors such as ecological competition may continue to select for those capacities. As new genomes and tools for analyzing molecular evolution become available, these questions become more tractable.

CONCLUSIONS

Understanding the paleoenvironmental information encoded in sulfur isotopes during sulfate reduction requires an understanding of how growth and physiology affect stable isotope fractionation (Bradley et al., 2011; Rees, 1973). De-convolving these effects becomes tractable through experimental and theoretical exploration, such as further elucidating the V_{max}/K_s relationship (A_s) with $K_{m\text{-}frac}$, which serves as a practical means of comparing fractionation data from different strains. It is clear that there is no unequivocal sulfate threshold concentration related to a step function in sulfur isotope fractionation across all strains, and it is unclear which strains, adapted to the modern environment, are the best proxies for Archaean microbial processes. Described here as a physiological and kinetic phenomenon, our framework for understanding fractionation helps explain recent observations of large $^{34}\varepsilon$ in low sulfate lake systems (Gomes and Hurtgen, 2013; Nakagawa et al., 2012). If the fractionation by MSR is in fact linked to multiple environmental and physiological variables, where each exhibit complex and non-linear (MM-like) responses, then articulating a clear heuristic for interpreting geological records is more challenging. Using sulfur isotopes to constrain sulfate concentrations in the Archean ocean is challenging, since the physiological parameters (affinity towards sulfate and electron donor) of Archaean microbes is unknown. Sulfate concentrations less than 200 μM are one explanation for small fractionations. It is also possible that small fractionations resulted from microbes with physiologies more like *D. alaskensis* than like *D. vulgaris.* Another alternative for small fractionations in Achaean seawater is that biological fractionations may have been large, but reservoir effects suppressed fractionation through reservoir effects {Crowe, 2014 #4561}. Independent approaches for understanding the chemistry of Archean seawater (Jamieson et al., 2012) (Halevy et al., 2010; Halevy et al., 2012) can help constrain sulfate concentrations and

480 shed light on the interpretation of sulfur isotopes in light of both seawater chemistry and
481 evolution. A more complete understanding of the sulfur isotope record will rely on building a
482 better understanding of the relevant enzymes, their expression and isotope fractionation in
483 response to environmental variables, and their evolution over the course of Earth history.
484
485

ACKNOWLEDGMENTS

Many thanks to Gill Geesey and Inês Cardoso-Pereira for providing cultures of *D. alaskensis* G20 and *D. vulgaris* Hildenborough, respectively. Andy Masterson, Erin Beirne, and Madeline Higgins provided expert analytical assistance. The authors acknowledge funding from NASA Exobiology Grant NNX07AV51G (to AHK, PRG and DTJ), NASA Astrobiology Institute (DTJ, AHK), the Microbial Sciences Initiative at Harvard (DTJ), NSF EAR Instrument and Facilities as well as Low Temperature Geochemistry and Geobiology (to DTJ), NSF Graduate Research Fellowship (WDL) and the Agouron Institute (ASB).

SUPPLEMENTAL INFORMATION:

Materials & Methods

Supplemental File 1 – *D. vulgaris* growth data

Supplemental File 2 – *D. alaskensis* growth data

REFERENCES CITED

Aksnes, D.L., Egge, J.K., 1991. A theoretical model for nutrient uptake in phytoplankton. Marine Ecology Progress Series 70, 65-72.

Bak, F., Pfennig, N., 1991. MICROBIAL SULFATE REDUCTION IN LITTORAL SEDIMENT OF LAKE CONSTANCE. Fems Microbiology Ecology 85, 31-42.

Berner, R.A., Canfield, D.E., 1989. A new model for atmospheric oxygen over Phanerozoic time. American Journal of Science 289, 333-361.

Bradley, A.S., Leavitt, W.D., Johnston, D.T., 2011. Revisiting the dissimilatory sulfate reduction network. Geobiology 9, 446-457.

Button, D.K., 1985. Kinetics of nutrient-limited transport and microbial growth. Microbiological reviews 49, 270-297.

Canfield, D., E., 2001. Isotope fractionation by natural populations of sulfate-reducing bacteria. 65, 1117-1124.

Canfield, D.E., 2004. The evolution of the Earth surface sulfur reservoir. American Journal of Science 304, 839-861.

Canfield, D.E., Farquhar, J., Zerkle, A.L., 2010. High isotope fractionations during sulfate reduction in a low-sulfate euxinic ocean analog. Geology 38, 415-418.

Canfield, D.E., Olesen, C.A., Cox, R.P., 2006. Temperature and its control of isotope fractionation by a sulfate-reducing bacterium. Geochimica et Cosmochimica Acta 70, 548-561.

Chambers, L.A., Trudinger, P.A., 1975. Are thiosulfate and trithionate intermediates in dissimilatory sulfate reduction? Journal of Bacteriology 123, 36-40.

Chambers, L.A., Trudinger, P.A., Smith, J.W., Burns, M.S., 1975. Fractionation of sulfur isotopes by continuous cultures of *Desulfovibrio desulfuricans*. Canadian Journal of Microbiology 21, 1602-1607.

Crowe, S.A., Paris, G., Katsev, S., Jones, C., Kim, S.-T., Zerkle, a.L., Nomosatryo, S., Fowle, D.A., Adkins, J.F., Sessions, A.L., Farquhar, J., Canfield, D.E., 2014. Sulfate was a trace constituent of Archean seawater. Science 346, 735-739.

Cypionka, H., 1995. Solute transport and cell energetics. In: L. Barton (Ed.), *Sulfate-Reducing Bacteria*, pp. 151-184. Plenum Press, New York.

Dalsgaard, T., Bak, F., 1994. NITRATE REDUCTION IN A SULFATE-REDUCING BACTERIUM, DESULFOVIBRIO-DESULFURICANS, ISOLATED FROM RICE PADDY SOIL - SULFIDE INHIBITION, KINETICS, AND REGULATION. Applied and environmental microbiology 60, 291-297.

Desmond-Le Quéméner, E., Bouchez, T., 2014. A thermodynamic theory of microbial growth. The ISME Journal 8, 1747-1751.

Farquhar, J., Johnston, D.T., Wing, B.A., Habicht, K.S., Canfield, D.E., Airieau, S., Thiemens, M.H., 2003. Multiple sulphur isotopic interpretations of biosynthetic pathways: implications for biological signatures in the sulphur isotope record. Geobiology 1, 27-36.

Fukui, M., Takii, S., 1994. Kinetics of sulfate respiration by free-living and particle-associated sulfate-reducing bacteria. Fems Microbiology Ecology 13, 241-247.

Gomes, M.L., Hurtgen, M.T., 2013. Sulfur isotope systematics of a euxinic, low-sulfate lake: evaluating the importance of the reservoir effect in modern and ancient oceans. Geology 41, 663-666.

546 Grein, F., Ramos, A.R., Venceslau, S.S., Pereira, I.A.C., 2013. Unifying concepts in anaerobic
547 respiration: insights from dissimilatory sulfur metabolism. Biochimica et Biophysica
548 Acta 1827, 145-160.
549 Habicht, K.S., Gade, M., Thamdrup, B., Berg, P., Canfield, D.E., 2002. Calibration of sulfate
550 levels in the Archean Ocean. Science 298, 2372-2374.
551 Habicht, K.S., Salling, L., Thamdrup, B., Canfield, D.E., 2005. Effect of Low Sulfate
552 Concentrations on Lactate Oxidation and Isotope Fractionation during Sulfate Reduction
553 by Archaeoglobus fulgidus Strain Z. Applied and environmental microbiology 71, 3770-
554 3777.
555 Halevy, I., Johnston, D.T., Schrag, D.P., 2010. Explaining the structure of the Archean mass-
556 independent sulfur isotope record. Science 329, 204-207.
557 Halevy, I., Peters, S.E., Fischer, W.W., 2012. Sulfate Burial Constraints on the Phanerozoic
558 Sulfur Cycle. Science (New York, NY) 337, 331-334.
559 Hansen, T., 1994. Metabolism of sulfate-reducing prokaryotes. Antonie van Leeuwenhoek 66,
560 165-185.
561 Harrison, A., Thode, H., 1958. Mechanism of the bacterial reduction of sulphate from isotope
562 fractionation studies. Transactions of the Faraday Society 54, 84-92.
563 Hauser, L.J., Land, M.L., Brown, S.D., Larimer, F., Keller, K.L., Rapp-Giles, B.J., Price, M.N.,
564 Lin, M., Bruce, D.C., Detter, J.C., Tapia, R., Han, C.S., Goodwin, L.A., Cheng, J.F.,
565 Pitluck, S., Copeland, A., Lucas, S., Nolan, M., Lapidus, A.L., Palumbo, A.V., Wall, J.D.,
566 2011. Complete Genome Sequence and Updated Annotation of Desulfovibrio alaskensis
567 G20. Journal of Bacteriology 193, 4268-4269.
568 Hayes, J.M., Waldbauer, J.R., 2006. The carbon cycle and associated redox processes through
569 time. Philosophical Transactions of the Royal Society B-Biological Sciences 361, 931-
570 950.
571 Healey, F.P., 1980. Slope of the Monod equation as an indicator of advantage in nutrient
572 competition. Microbial Ecology 5, 281-286.
573 Heidelberg, J.F., Seshadri, R., Haveman, S.A., Hemme, C.L., Paulsen, I.T., Kolonay, J.F., Eisen,
574 J.A., Ward, N., Methé, B., Brinkac, L.M., Daugherty, S.C., Deboy, R.T., Dodson, R.J.,
575 Durkin, A.S., Madupu, R., Nelson, W.C., Sullivan, S.A., Fouts, D., Haft, D.H., Selengut,
576 J., Peterson, J.D., Davidsen, T.M., Zafar, N., Zhou, L., Radune, D., Dimitrov, G., Hance,
577 M., Tran, K., Khouri, H., Gill, J., Utterback, T.R., Feldblyum, T.V., Wall, J.D.,
578 Voordouw, G., Fraser, C.M., 2004. The genome sequence of the anaerobic, sulfate-
579 reducing bacterium Desulfovibrio vulgaris Hildenborough. Nature Biotechnology 22,
580 554-559.
581 Holmer, M., Storkholm, P., 2001. Sulphate reduction and sulphur cycling in lake sediments: a
582 review. Freshwater Biology 46, 431-451.
583 Ingvorsen, K., Jørgensen, B.B., 1984. Kinetics of sulfate uptake by freshwater and marine
584 species of *Desulfovibrio*. Archives of Microbiology 139, 61-66.
585 Ingvorsen, K., Zehnder, A.J.B., Jorgensen, B.B., 1984. KINETICS OF SULFATE AND
586 ACETATE UPTAKE BY DESULFOBACTER-POSTGATEI. Applied and
587 environmental microbiology 47, 403-408.
588 Jamieson, J.W., Wing, B.A., Farquhar, J., Hannington, M.D., 2012. Neoarchaean seawater
589 sulphate concentrations from sulphur isotopes in massive sulphide ore. Nature
590 Geoscience 6, 61-64.

591 Johnston, D., Farquhar, J., Canfield, D., 2007. Sulfur isotope insights into microbial sulfate
592 reduction: When microbes meet models. Geochimica et Cosmochimica Acta 71, 3929-
593 3947.
594 Johnston, D.T., Farquhar, J., Wing, B.A., Kaufman, A.J., Canfield, D.E., Habicht, K.S., 2005.
595 Multiple sulfur isotope fractionations in biological systems: A case study with sulfate
596 reducers and sulfur disproportionators. American Journal of Science 305, 645-660.
597 Jorgensen, B.B., 1979. Theoretical model of the stable isotope distribution in marine sediments.
598 Geochimica et Cosmochimica Acta 43, 363-374.
599 Kaplan, I., Rittenberg, S., 1964. Microbiological fractionation of sulfur isotopes. Journal of
600 General Microbiology 34, 195-&.
601 Laws, E.A., Popp, B.N., Bidigare, R.R., Kennicutt, M.C., Macko, S.A., 1995. Dependence of
602 phytoplankton carbon isotopic composition on growth rate and [CO2]aq: theoretical
603 considerations and experimental results. Geochimica et Cosmochimica Acta 59, 1131-8.
604 Leavitt, W.D., Halevy, I., Bradley, A.S., Johnston, D.T., 2013. Influence of sulfate reduction
605 rates on the Phanerozoic sulfur isotope record. Proceedings of the National Academy of
606 Sciences, in press.
607 Nakagawa, M., Ueno, Y., Hattori, S., Umemura, M., Yagi, A., Takai, K., Koba, K., Sasaki, Y.,
608 Makabe, A., Yoshida, N., 2012. Seasonal change in microbial sulfur cycling in
609 monomictic Lake Fukami-ike, Japan. Limnology and Oceanography 57, 974-988.
610 Okabe, S., Nielsen, P.H., Characklis, W.G., 1992. FACTORS AFFECTING MICROBIAL
611 SULFATE REDUCTION BY DESULFOVIBRIO-DESULFURICANS IN
612 CONTINUOUS CULTURE - LIMITING NUTRIENTS AND SULFIDE
613 CONCENTRATION. Biotechnology and Bioengineering 40, 725-734.
614 Pallud, C., Van Cappellen, P., 2006. Kinetics of microbial sulfate reduction in estuarine
615 sediments. Geochimica Et Cosmochimica Acta 70, 1148-1162.
616 Pereira, I.A.C., Ramos, A.R., Grein, F., Marques, M.C., da Silva, S.M., Venceslau, S.S.,
617 2011. A comparative genomic analysis of energy metabolism in sulfate reducing
618 bacteria and archaea. Frontiers in Microbiology 2, Article 69.
619 Piłsyk, S., Paszewski, A., 2009. Sulfate permeases—phylogenetic diversity of sulfate transport.
620 Acta Biocimica Polonica 56, 375-384.
621 Popp, B.N., Laws, E.A., Bridigare, R.R., Dore, J.E., Hanson, K.L., Wakeham, S.G., 1998. Effect
622 of phytoplankton cell geometry on carbon isotopic fractionation. Geochimica et
623 Cosmochimica Acta 62, 69-77.
624 Rees, C.E., 1973. Steady-state model for sulfur isotope fractionationin bacterial reduction
625 processes. Geochimica et Cosmochimica Acta 37, 1141-1162.
626 Roychoudhury, A.N., 2004. Sulfate respiration in extreme environments: A kinetic study.
627 Geomicrobiology Journal 21, 33-43.
628 Saito, M.A., Goepfert, T.J., Ritt, J.T., 2008. Some thoughts on the concept of colimitation: Three
629 definitions and the importance of bioavailability. Limnology and Oceanography 53, 276-
630 290.
631 Sim, M.S., Bosak, T., Ono, S., 2011a. Large Sulfur Isotope Fractionation Does Not Require
632 Disproportionation. Science (New York, NY) 333, 74-77.
633 Sim, M.S., Ono, S., Bosak, T., 2012. Effects of Iron and Nitrogen Limitation on Sulfur Isotope
634 Fractionation during Microbial Sulfate Reduction. Applied and environmental
635 microbiology 78, 8368-8376 %R 10.1128/AEM.01842-12.

636 Sim, M.S., Ono, S., Donovan, K., Templer, S.P., Bosak, T., 2011c. Effect of electron donors on
637 the fractionation of sulfur isotopes by a marine *Desulfovibrio* sp. Geochimica et
638 Cosmochimica Acta 75, 4244-4259.
639 Smith, S.L., Yamanaka, Y., Pahlow, M., Oschlies, A., 2009. Optimal uptake kinetics:
640 physiological acclimation explains the pattern of nitrate uptake by phytoplankton in the
641 ocean. Marine Ecology Progress Series 384, 1-12.
642 Szabo, A., Tudge, A., Macnamara, J., Thode, H.G., 1950. The distribution of S-34 in nature and
643 the sulfur cycle. Science 111, 464-465.
644 Tarpgaard, I.H., Røy, H., Jørgensen, B.B., 2011. Concurrent low- and high-affinity sulfate
645 reduction kinetics in marine sediment. Geochimica et Cosmochimica Acta 75, 2997-3010.
646 Tcherkez, G.G.B., Farquhar, G.D., Andrews, T.J., 2006. Despite slow catalysis and confused
647 substrate specificity, all ribulose bisphosphate carboxylases may be perfectly optimized.
648 Proceedings of the National Academy of Sciences 103, 7246-7251.
649 Venceslau, S.S., Stockdreher, Y., Dahl, C., Pereira, I.A.C., 2014. The "bacterial heterodisulfide"
650 DsrC is a key protein in dissimilatory sulfur metabolism. Biochimica et Biophysica Acta
651 1837, 1148-1164.
652 Wall, J.D., Rapp-Giles, B.J., Rousset, M., 1993. Characterization of a small plasmid from
653 *Desulfovibrio desulfuricans* and its use for shuttle vector construction. Journal of
654 Bacteriology 1775, 4121-4128.
655 Wing, B.A., Halevy, I., 2014. The sulfur isotope phenotypes of sulfate-respiring bacteria and
656 archaea. Proceedings of the National Academy of Sciences, in press.
657 Wu, N., Farquhar, J., 2011. Metabolic rates and sulfur cycling in teh geologic record.
658 Proceedings of the National Academy of Sciences 110, 11217-11218.
659 Zerkle, A.L., Farquhar, J., Johnston, D.T., Cox, R.P., Canfield, D.E., 2009. Fractionation of
660 multiple sulfur isotopes during phototrophic oxidation of sulfide and elemental sulfur by
661 a green sulfur bacterium. Geochimica et Cosmochimica Acta 73, 291-306.

662

663 **FIGURE CAPTIONS**

664

665 ***Figure 1***. **Sulfate concentrations in each chemostat experiment at steady-state and the**
666 **resulting strain-specific major isotope fractionation between sulfate and sulfide ($^{34}\varepsilon_{SO4/H2S}$).**
667 Samples for isotope measurements are taken at steady-state sulfate concentrations. Strain
668 *Desulfovibrio vulgaris* Hildenborough (red) exhibits larger isotope effects across the full range of
669 sulfate concentrations, whereas strain *Desulfovibrio alaskensis* strain G20 (blue) shows strong
670 concentration dependence.

671

672 ***Figure 2.*** **Triple isotope data for variable sulfate chemostat experiments.** The left y-axis
673 indicates $^{33}\lambda$, again plotted against $^{34}\boldsymbol{\varepsilon}$ for *D. vulgaris* (blue circles) and *D. alaskensis* (green
674 closed squares). The right y-axis shows $\Delta^{33}S$, plotted against $^{34}\boldsymbol{\varepsilon}$ for *D. vulgaris* (red open
675 circles) and *D. alaskensis* (red closed circles).

676

677 ***Figure 3.*** Comparison between our data (*D. vulgaris* in red and *D. alaskensis* in blue) and those
678 generated in a semi-continuous culture apparatus by Habicht et al. (2002, 2005) (in black
679 symbols), along with values from *D. desulphuricans* (green) from Harrison and Thode, (1958),
680 from closed-system experiments. Data from Habicht et al. (2002, 2005) include enrichment
681 (mixed) cultures from freshwater (diamonds) and marine (squares) environments, as well as pure
682 culture studies on the hyperthermophilic Arcahaea, *Archaeoglobus fulgidis* strain Z (triangles).

683

684 ***Figure 4:*** The operation of sulfite reduction by Dsr: sulfite and electrons are supplied to the
685 enzyme DsrAB, which is complexed with DsrC. Partially reduced sulfur is removed by DsrC,
686 which cycles to membrane-bound DsrMKJOP where cellular energy is conserved. During this
687 cycle, reduced S is released as H_2S.

688

689 ***Figure 5*****: The relationship between sulfate concentration, csSRR, and expressed isotope**
690 **fractionation.** A) relationship between sulfate concentration and isotope fractionation for a
691 variety of sulfate reduction rates. The maximum fractionation at lowest csSRR approaches the
692 equilibrium isotope fractionation between sulfate and sulfide. Concentrations are expressed in
693 multiples of $K_{m\text{-}frac}$. B) Relationship between maximum fractionation and csSRR, for a variety of

sulfate concentrations. the x-axis in (B) is equivalent to a vertical line intersecting the x-axis in (A). *inset* shows the relationship between the curves at different concentrations. This relationship follows a Monod curve (A).

Figure 6: **Four ecological regimes relevant to sulfur isotope fractionation.** The x-axis indicates increasing sulfate concentration while y-axis indicates increasing electron donor concentration. In growth under sulfate limitation, electron donor is in excess and fractionation is low. In growth under electron donor limitation, a large fractionation is expected, primarily as a function of slow growth. Co-limitation of sulfate and electron donor is likely to produce a complex physiological pattern that is not well understood. Nutrient or other growth limitation (e.g. temperature) suggests that both sulfate and donor will be abundant (as is typical at the beginning of batch growth experiments); isotope fractionations are expected to be intermediate in magnitude. Boundaries between these regimes are not sharp, and are expected to relate to the cellular affinity (A_s) for these substrates.

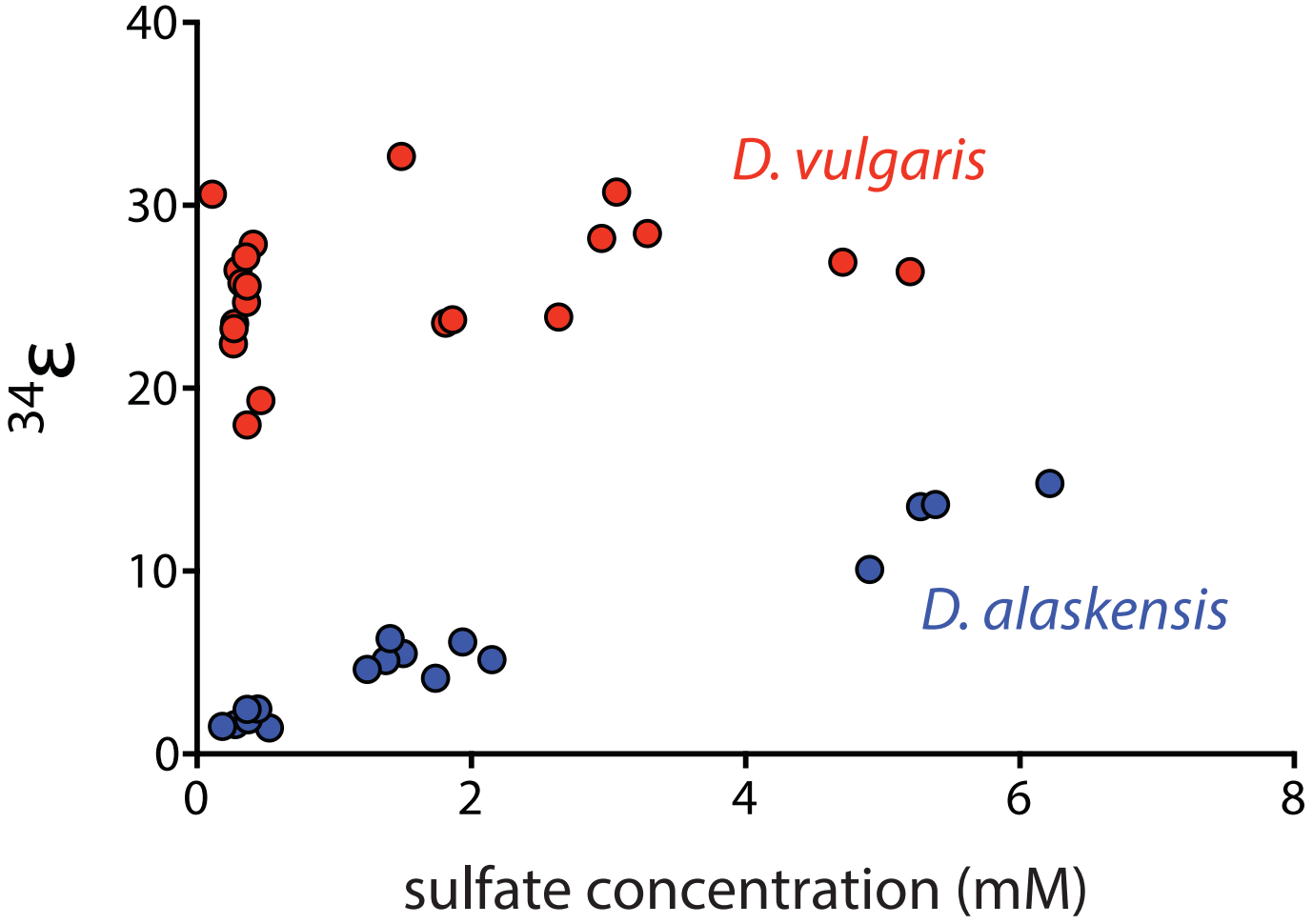
40
30
20
10
0
0
2
4
6
8
34ε
D. vulgaris
D. alaskensis
sulfate concentration (mM)

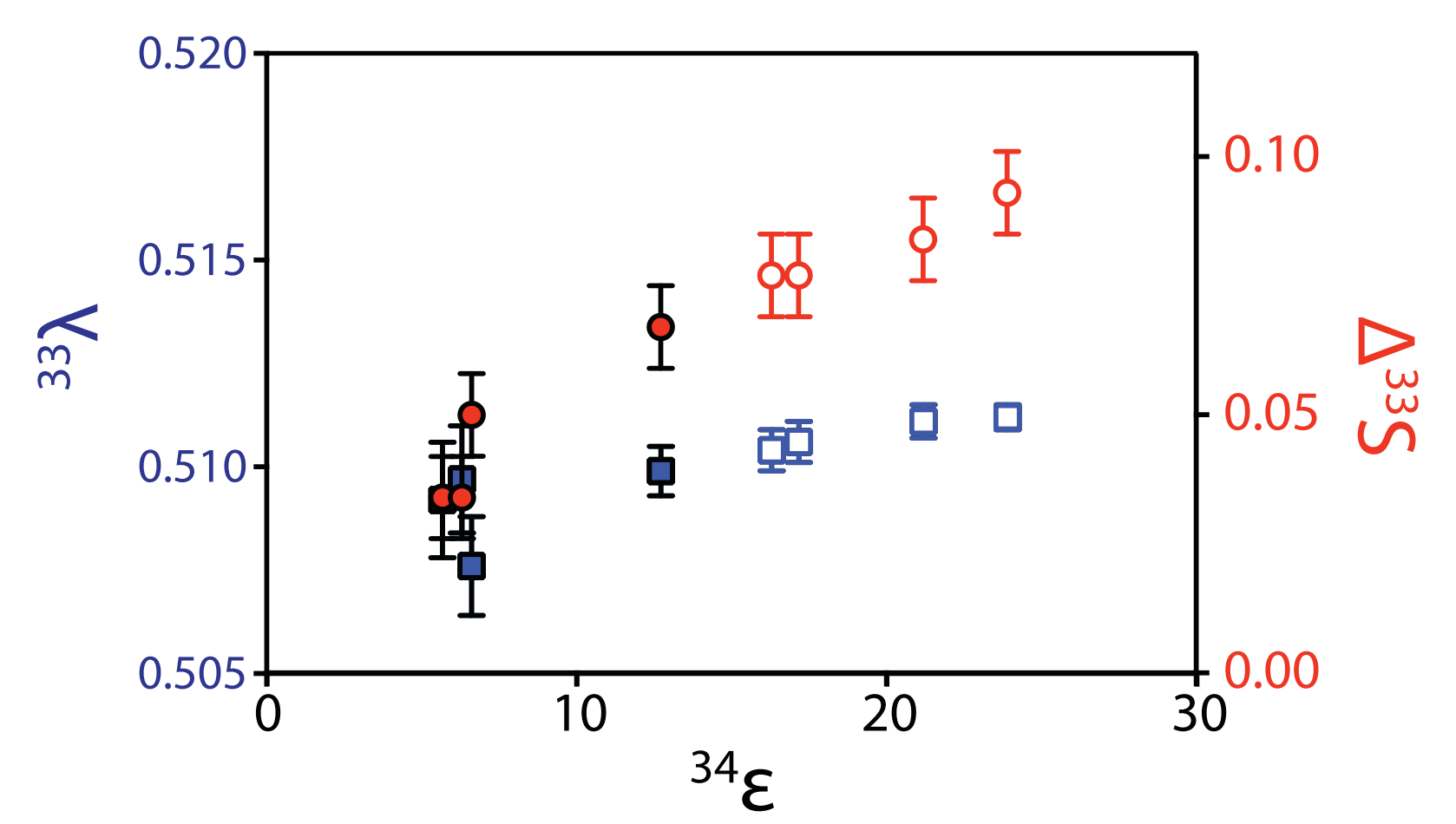
0.520
0.515
0.510
0.505
γ_{33}
0.10
0.05
0.00
$\Delta^{33}S$
0
10
20
30
$^{34}\varepsilon$

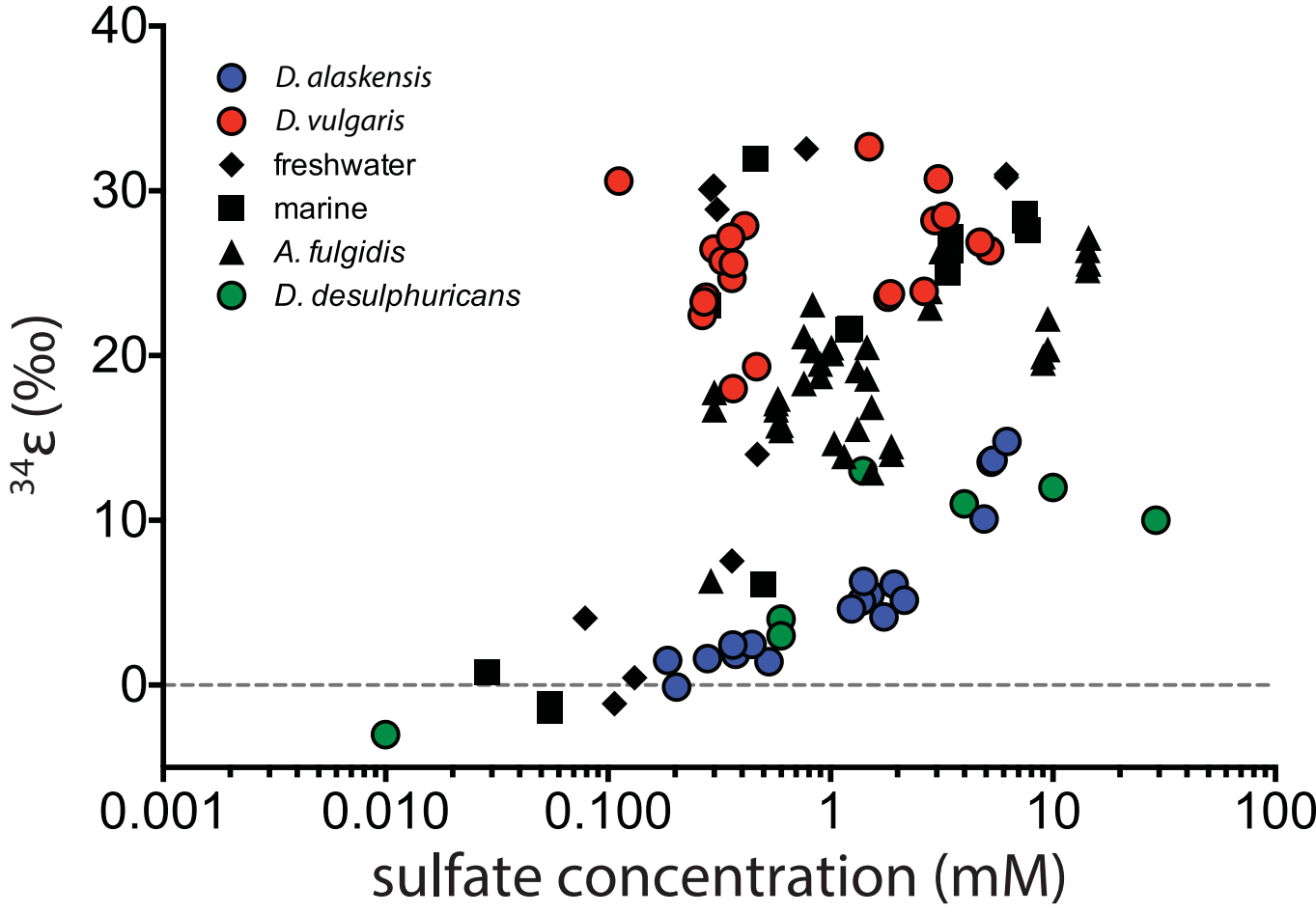
40
30
20
10
0
$^{34}\varepsilon$ (‰)
D. alaskensis
D. vulgaris
freshwater
marine
A. fulgidis
D. desulphuricans
0.001
0.010
0.100
1
10
100
sulfate concentration (mM)

FIGURE 3

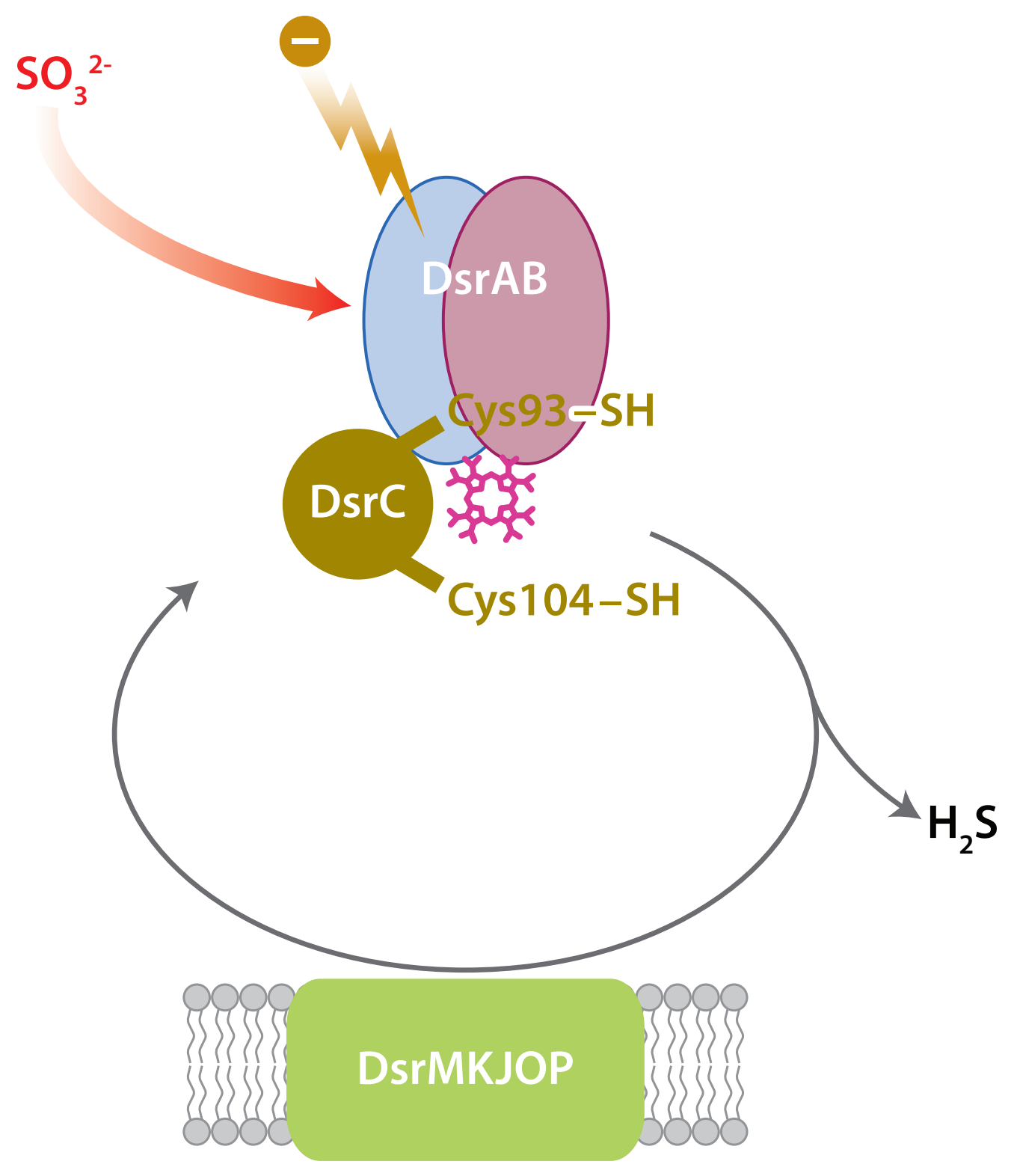
SO_3^{2-}
DsrAB
Cys93–SH
DsrC
Cys104–SH
H_2S
DsrMKJOP

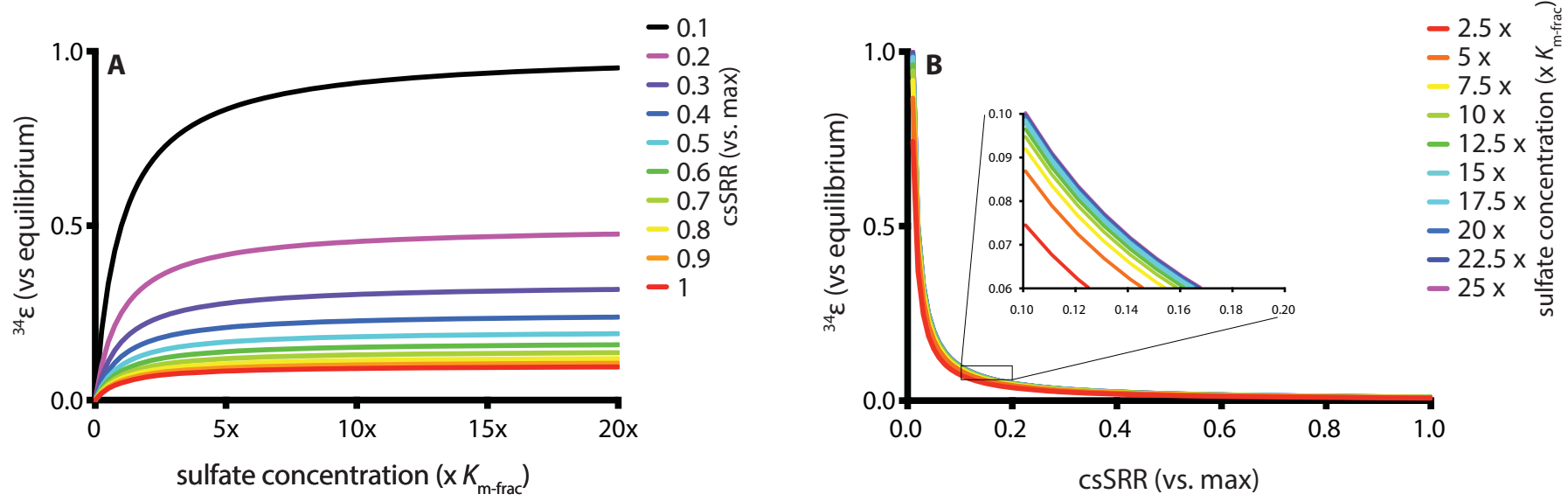
A
B
1.0
0.5
0.0
0
5x
10x
15x
20x
sulfate concentration (x $K_{m\text{-}frac}$)
$^{34}\varepsilon$ (vs equilibrium)
csSRR (vs. max)
0.1
0.2
0.3
0.4
0.5
0.6
0.7
0.8
0.9
1
2.5 x
5 x
7.5 x
10 x
12.5 x
15 x
17.5 x
20 x
22.5 x
25 x
sulfate concentration (x $K_{m\text{-}frac}$)
0.10
0.09
0.08
0.07
0.06
0.10
0.12
0.14
0.16
0.18
0.20
0.0
0.2
0.4
0.6
0.8
1.0

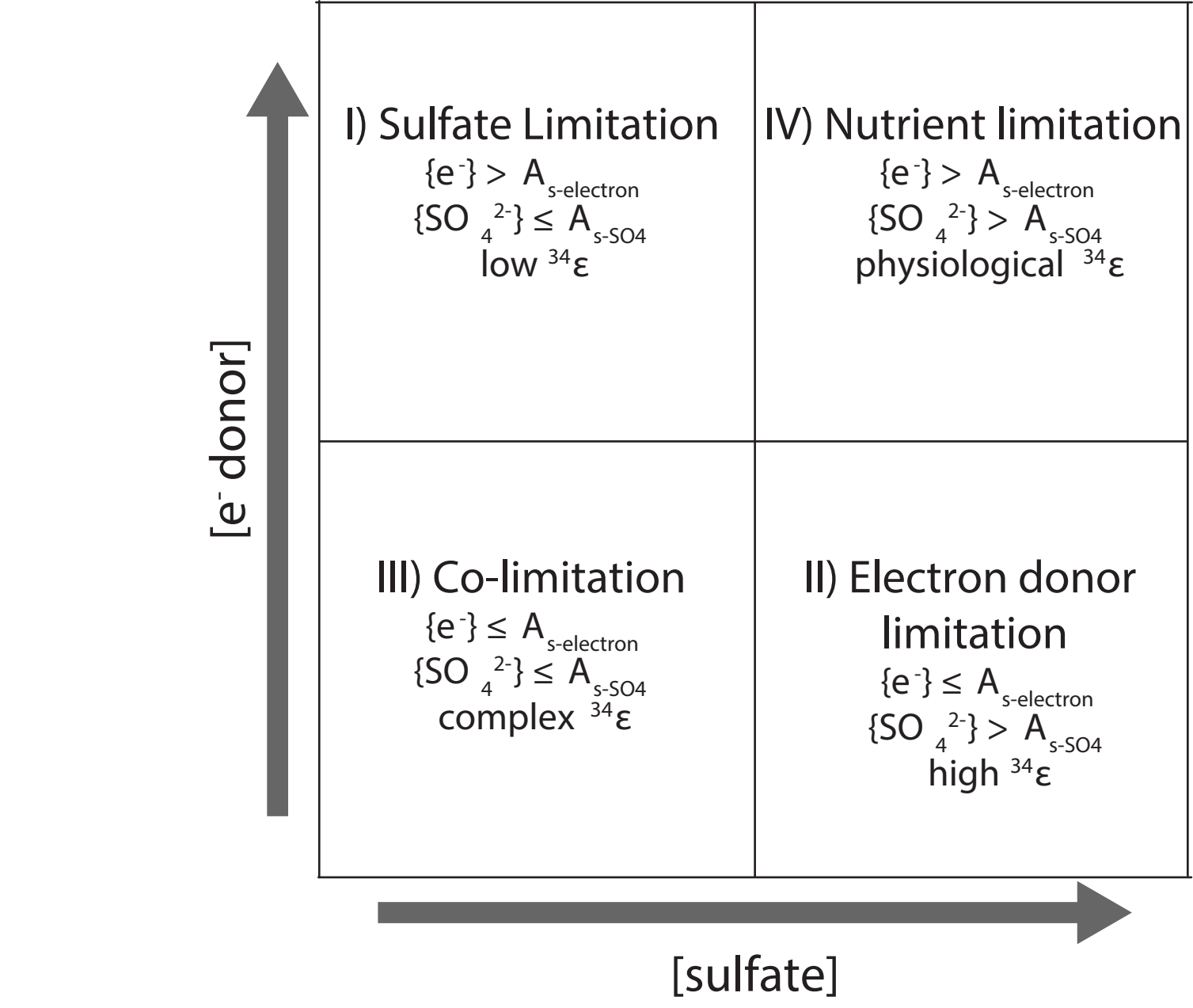
I) Sulfate Limitation
{e-} > A s-electron
{SO 4 2-} ≤ A s-SO4
low 34ε
IV) Nutrient limitation
{e-} > A s-electron
{SO 4 2-} > A s-SO4
physiological 34ε
III) Co-limitation
{e-} ≤ A s-electron
{SO 4 2-} ≤ A s-SO4
complex 34ε
II) Electron donor limitation
{e-} ≤ A s-electron
{SO 4 2-} > A s-SO4
high 34ε
[e- donor]
[sulfate]

FIGURE 4